Dear Author:

Attached you will find a pdf of the proofs of your article scheduled to appear in a forthcoming issue of *Neural Computation*.

Please print out the pdf of your proof on standard size paper (8 ½ x 11) single-sided, and check for accuracy and consistency, making especially sure to check the accuracy of material that only you can verify (such as numerical data or spelling of proper names). Please also check all figures on the proofs for orientation, legibility, and overall quality and initial your approval next to all figures. Throughout, please limit your changes to those necessary to correct errors or inconsistencies. Major changes to the manuscript or replacement of figures may not be made. Note that changes resulting in repagination of the issue will not be accepted. Please do not send a revision of your article and do not alter the pdf that was sent to you. If you are unable to get the corrections back to us within the requested time frame, we can not guarantee that your changes will be incorporated.

Please mark corrections in red pen directly on the proofs. Please also include a typed list detailing changes. If each figure is approved please indicate this on the list. If you are not approving the figures and new figures have been sent, please indicate why. Please send only one set of corrections on one master copy and one list of changes, even if there is more than one author making changes.

Within three days of receipt of the email notification, please use an overnight delivery service to send your corrected proofs and detailed list to the contact below.

Should you decide to fax or email your corrections, please be sure to provide the following:

- A list containing all changes, including figure approval.
- A copy of every page and figure where corrections are marked.
- If, because of error in placement or reproduction, adjustments to figures are required or new figures are sent, include on the list of changes an explanation of why this is necessary.

Contact Information:
Eric Witz
MIT Press Journals
238 Main St., Suite 500
Cambridge, MA 02142-1046
Email: ewitz@mit.edu
Phone: (617) 258-0586
Fax: (617) 258-5028

Thank you for your cooperation.

Yours sincerely,

Eric Witz
Production Coordinator
MIT Press Journals
Email: ewitz@mit.edu

ARTICLE **Communicated by Emilio Salinas**

Saccade Updating by Vector Subtraction: Analysis of Multiplicative Gain Field Models

Carlos R. Cassanello
cc2391@columbia.edu
Vincent P. Ferrera
vpf3@columbia.edu
Columbia University, Department of Psychiatry, Center for Neurobiology and Behavior, David Mahoney Center for Brain and Behavior Research, New York, NY 10032, U.S.A.

Saccadic eye movements remain spatially accurate even when the target becomes invisible and the initial eye position is perturbed. The computation that underlies this accuracy is approximated by vector subtraction: the original saccade vector is updated by subtracting the vector corresponding to the intervening eye movement. The neural mechanism by which vector subtraction is implemented is not fully understood. Here, we investigate vector subtraction within a framework in which eye position and retinal target position signals interact multiplicatively (gain field). When the eyes move, they induce a spatial modulation of the firing rates across a retinotopic map of neurons. The updated saccade metric can be read from the shift of the peak of the population activity across the map. This model uses a quasi-linear (half-rectified) dependence on the eye position and requires the slope of the eye position input to be negatively proportional to the preferred retinal position of each neuron. We derive analytically this constraint and study its range of validity. We discuss how this mechanism relates to experimental results reported in the frontal eye fields of macaque monkeys.

1 Introduction

The retinal image of an object changes whenever the object moves or the eyes move. However, monkeys and humans are able to saccade accurately to the remembered location of a target that has been rendered invisible even when there is an intervening shift of gaze between the target's disappearance and the final saccade. The brain accomplishes this by updating the displacement needed to acquire the target based on the most recent position of the eyes. This displacement can be approximated as a vector subtraction between the retinal representation of the location of the target at the instant it was perceived and the change in eye position. This computation requires that the brain integrate the retinal position of a target stimulus with the eye

Neural Computation **19, 1–33** (2007)

position in order to acquire the target. In this article, we discuss a way of performing this updating online by vector subtraction.

There is substantial evidence that retinal and eye position signals interact multiplicatively in several regions of visual cortex (Andersen & Mountcastle, 1983; Andersen, Essick, & Siegel, 1985; Andersen, Bracewell, Barash, Gnadt, & Fogassi, 1990; Van Opstal, Hepp, Suzuki, & Henn, 1995; Campos, Cherian, & Segraves, 2006). Updating saccade plans in multiplicative gain field models is not straightforward, and most previous approaches have used neural networks (Zipser & Andersen, 1988; Salinas & Abbott, 1995, 1997; Pouget & Sejnowski, 1997; Xing & Andersen, 2000; Quaia, Opticon, & Goldberg, 1998; Mitchell & Zipser, 2003; Pouget & Snyder, 2000; but see also Siegel, 1998). Although these networks achieve the appropriate transformation, an analytical approach can provide insight into how this is accomplished. The approach taken here is similar in that we start with the goal of the computation: to perform vector subtraction. However, instead of constructing a network, we use analytic methods to derive a minimal model that solves the problem. The goal of this study is to derive analytic solutions for computing saccade updating by vector subtraction in a population of neurons with gain field–like properties. We discuss the conditions that need to be imposed on the gain field in order to do this computation at a single-neuron level given certain assumptions, and we show using simple simulations how these conditions may be implemented by the neuronal hardware.

2 Results

2.1 Gain Field Differential Equation and Gain Field Modulation Model. The problem to be solved is shown in Figure 1. The eyes are fixating at FP1 when a target is momentarily presented. After the target disappears, the eyes move to FP2. This is the first step of a double-step saccade, the ultimate goal of which is to acquire the remembered location of the target. The vector of the saccade required for the second step needs to be updated based on the information provided by $\boldsymbol{x}$ and $\boldsymbol{y}$, which represent retinal target position (RTP) and eye position (EP), respectively. Both $\boldsymbol{x}$ and $\boldsymbol{y}$ are measured relative to the first fixation position (FP1).

The model does not incorporate any time dependence in the response of the neurons. It is assumed that the response to the initial target presentation is sustained after the target disappears. It is this sustained memory or motor-plan-related activity that is modulated by eye position. It is further assumed that the target is briefly presented and that all subsequent behavior occurs in total darkness.

The model takes as inputs the retinal target position given by $\boldsymbol{x}$ and the change in eye position denoted $\boldsymbol{y}$ before the final saccade (see Figure 1). The

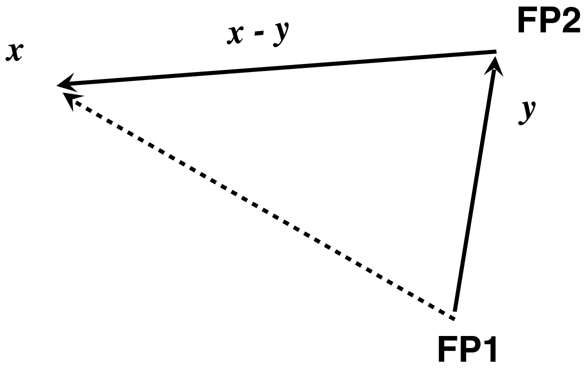

Figure 1: Memory-guided saccade with intervening gaze shift (double-step saccade). The subject fixates at FP1 when the target is flashed at location $\boldsymbol{x}$. Eye movements are shown with solid black arrows. After the target is turned off and before the second saccade, there is a shift in gaze by an eye position displacement in the dark given by $\boldsymbol{y}$. To accurately acquire the target ($\boldsymbol{x}$), the second saccade needs to be updated to the vector difference $\boldsymbol{x} - \boldsymbol{y}$.

output is the saccade vector $\boldsymbol{x} - \boldsymbol{y}$. Each model cell has a response of the general form

$$R(x, y, \rho) = f(x, \rho) \bullet g(y, \rho). \tag{2.1}$$

Here f is a retinal sensitivity function, and g is the eye position sensitivity function that modulates the retinal input; $\boldsymbol{\rho}$ denotes the center of the retinal receptive fields of neurons in the model. Saccade direction and amplitude are encoded by the location of the peak response of a population of model neurons. Therefore, for a saccade of amplitude $(x - y)_0$, the response R must have a maximum over the variable $\boldsymbol{\rho}$ at the location of those cells for which $\boldsymbol{\rho}_0 = (x - y)_0$. Given a particular form for the retinal sensitivity function $f(\boldsymbol{x},\rho)$, the eye position sensitivity function $g(\boldsymbol{y},\rho)$ that satisfies the vector subtraction constraint can be derived by finding the maximum of R with respect to the preferred retinal location ($\boldsymbol{\rho}$). Since R is given by the product of f and g, g must obey the following differential equation,

$$\frac{\partial}{\partial\rho}\log\ g|_y = -\frac{\partial}{\partial\rho}\log\ f|_x = -\frac{1}{\sigma^2}\bullet(x-\rho) \quad \equiv \quad -\frac{1}{\sigma^2}\bullet y, \tag{2.2}$$

where the last identity in the right-hand side of equation 2.2 enforces the constraint $\boldsymbol{\rho} = \boldsymbol{x} - \boldsymbol{y}$ in order to obtain a function of only $\boldsymbol{y}$ and ρ. We call this the vector subtraction condition. The structure of equation 2.2 is a consequence of the assumptions of a multiplicative modulation and the independence of the variables.

The vector subtraction constraint allows one to obtain a closed differential equation, which can be solved for g. When $f(x, \rho)$ is a gaussian receptive field of size $\boldsymbol{\sigma}$ entered at $\boldsymbol{\rho}$

$$f(x, \rho) \; = f_0 \frac{1}{\sqrt{2\pi}\sigma} \exp\left(-\frac{1}{2\sigma^2}(x-\rho)^2\right), \tag{2.3}$$

the derived eye position sensitivity function has the form

$$g(y, \rho) \; = g_0 \bullet \exp\left(-\frac{\rho}{\sigma^2} \bullet y\right) \approx g_0 \bullet \left[1 - \frac{\rho}{\sigma^2} \bullet y + \cdots\right]_+ . \tag{2.4}$$

Together $f(x,\rho)$ and $g(y,\rho)$ describe the responses of a population of neurons that form a saccade vector map in retinotopic coordinates. Saccade vectors are encoded by the peak of the population response. This peak moves as the eyes move to update the saccade command. This solution is unique up to an arbitrary function of $\boldsymbol{x}$ and y. The $+$ subscript on the right-hand side of equation 2.4 indicates that under certain conditions to be specified, we can approximate the exponential gain field by the linear rectified term of its polynomial expansion.

What is important from the standpoint of vector subtraction is not only the functional form of $\boldsymbol{g}(\boldsymbol{y},\rho)$, but the relationship between the parameters in $\boldsymbol{g}(\boldsymbol{y},\rho)$ and $\boldsymbol{f}(\boldsymbol{x},\rho)$. For each cell, the preferred retinal location, $\boldsymbol{\rho}$, and size of the receptive field, $\boldsymbol{\sigma}$, determine the slope of the eye position sensitivity function. Across the population, the slope of the eye position sensitivity function increases in magnitude with the eccentricity of the receptive field center but is opposite in sign.

The same strategy can be applied to other receptive field shapes. If the visual receptive field is modeled as a sigmoid,

$$f(x, \rho) \; = \frac{A}{2} \bullet \left[1 + \tanh\left(\frac{x-\rho}{\eta}\right)\right], \tag{2.5}$$

where A is the amplitude of the neuron's response, $\boldsymbol{\rho}$ is the point where the visual response reaches half of its amplitude, and $\boldsymbol{\eta}$ is the half-width of the spatial rise of the receptive field, the companion eye position sensitivity function results:

$$g(y, \rho) \; = g_0 \bullet \exp\left[\left(1 - \tanh\left(\frac{y}{\eta}\right)\right) \bullet \frac{\rho}{\eta}\right] \cong g_0 \bullet \left[1 - y \bullet \frac{\rho}{\eta^2} + \cdots\right]_+ . \tag{2.6}$$

We can pick g_0 to be $\exp(-\frac{\rho}{\eta})$ so that $g(\boldsymbol{y} = \boldsymbol{0}, \rho) = 1$.

For both gaussian and sigmoidal receptive fields, the derived eye position sensitivity function is an exponential function of eye position. The exponential function implements the mapping of an additive structure into a multiplicative one, which allows the model to take into account successive gaze shifts. However, the brain can compute an approximate vector subtraction using a linear rectified approximation to the exponential gain field function. This approximation, which uses the right-hand side of equations 2.4 and 2.6, is used in the model simulations, and its validity is discussed in a later section.

2.2 Eye Position versus Eye Displacement. In the derivations above, $\boldsymbol{y}$ represents eye position relative to the center of gaze, which is identical to the primary position of the eye. When the eye is in this position, the eye position gain for all cells is 1.0. What happens if the animal performs a double-step saccade task where the initial fixation position (FP1) is at an eccentric location? In this case, $\boldsymbol{y}$ represents the change in eye position, FP2 − FP1, or eye displacement. In terms of the model presented above, it does not matter if $\boldsymbol{y}$ represents absolute eye position or eye displacement. The activity in the retinal map will shift by an amount $-\boldsymbol{y}$ in either case. However, there is an interesting wrinkle. If the input to the model encodes absolute eye position and the eyes start at an eccentric position, then the gain factor will vary across neurons depending on their eye position sensitivity functions. If eye position gain modulates visual responses, then the response to a visual target will be distorted whenever the animal is fixating eccentrically. Specifically, if a target is presented at position $\boldsymbol{x}_0$ while the eyes are at position $\boldsymbol{y}_0$, then the maximal activity across the population will be not at $\boldsymbol{x}_0$ but at $\boldsymbol{x}_0 - \boldsymbol{y}_0$. A full treatment of this case is beyond the scope of this article. However, one potential solution might be to incorporate temporal dynamics into the eye position sensitivity function such that whenever the eye starts in an eccentric position, all of the gains relax back to the initial, uniform state (e.g., all gains = 1.0). In this case, the model should behave as if the eye is always in primary position at the start of the task, regardless of the location of FP1. However, the eye position gains should not relax to a uniform state when the eye moves to FP2. Hence, the dynamics would need to be sensitive to behavioral state (i.e., fixating versus planning the next saccade). These considerations suggest that the eye position signal should not be a tonic representation of absolute eye position but a dynamic representation of eye displacement.

2.3 One-Dimensional Model Simulations. We simulate the response of a one-dimensional array of neurons with gaussian receptive fields, modulated by an eye position sensitivity function that has a quasi-linear (half-rectified) dependence on eye position. The coefficient of the eye position term is proportional to the receptive field eccentricity but with the opposite sign. All gain fields intersect at the center of gaze (see Figures 2A and 2B).

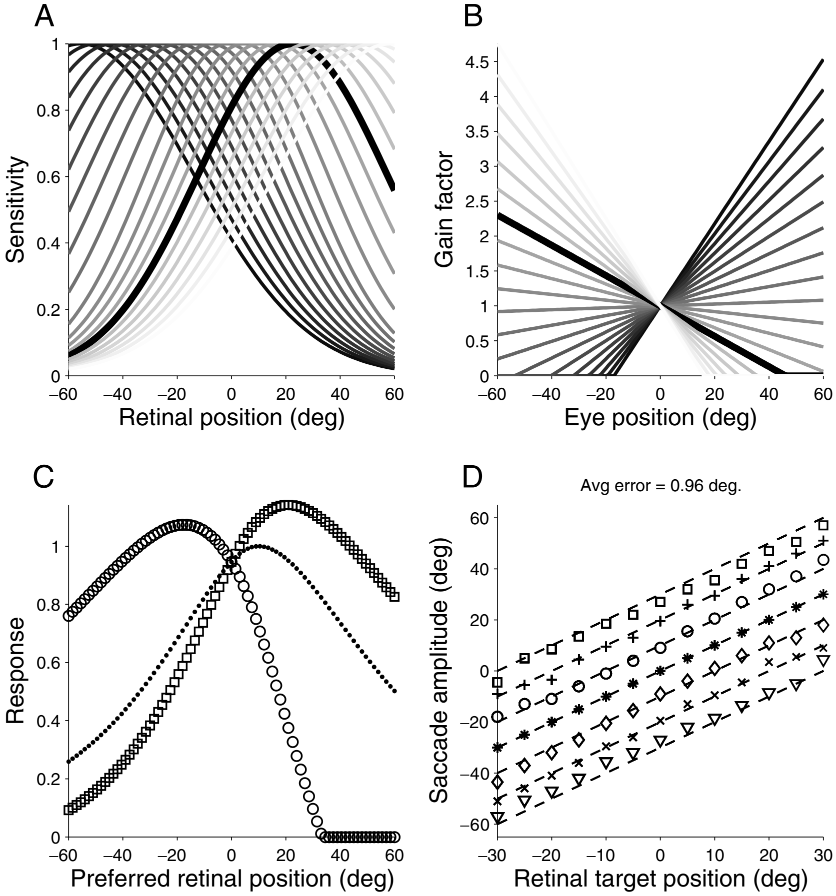

Figure 2: One-dimensional gain field model comprising an array of 81 neurons with gaussian receptive fields and quasi-linear gain fields. (A) Visual receptive fields of a subset of neurons. (B) Eye position sensitivity functions (gain fields) for the same neurons as in *A*. The darkness of the lines indicates the correspondence between the curves in *A* and *B*, for example, the heavy black curves represent the retinal and eye position sensitivity functions for the same neuron. (C) Population response for the three conditions: solid dots, initial target position = 10 degrees and eye position = 0; open squares, initial target position = 10 degrees and eye position = −10 degrees, requiring a 20 degree rightward saccade; open circles, initial target position = 10 degrees and eye position = 30 degrees, requiring a 20 degree leftward saccade. (D) Predicted second saccade amplitudes (symbols) compared to exact required update (dashed lines) for various initial target locations and eye positions, both ranging from −30 to 30 degrees in 10 degree steps. Each group of symbols represents saccade amplitude to various initial target locations for one particular eye position.

The array consists of 81 neurons with receptive fields equally spaced covering retinal positions within 60 degrees of the fovea. Each unit's response has the form

$$R(x, y, \rho) = A_1 \bullet \exp\left[-\frac{1}{2\sigma^2}(x-\rho)^2\right] \bullet [1 - A_2 \cdot \rho \cdot y]_+ . \tag{2.7}$$

Figure 2A shows the visual receptive fields of a subset of the units. Figure 2B shows the corresponding gain field functions, which have been half rectified. Figure 2C shows the population response for three different saccades: filled triangles represent a target 10 degrees to the right with initial eye position at the primary position; filled circles have initial eye position at 10 degrees to the left of the primary position with target flashed 10 degrees to the right of the fovea; and filled diamonds represent a target flashed at 10 degrees to the right of the fovea but the eyes shifted to 20 degrees to the right, therefore requiring a leftward saccade. The population response is always unimodal and peaks around the amplitude of the correct saccade amplitude and direction, indicating that the most active cells in the population are those with receptive field eccentricity congruent with the saccade.

Figure 2D shows the discrepancy between the center of the population activity (updated saccade vector) predicted by the model and the actual size of the ideal second-step saccade for various locations of the target. The diagonal dashed lines indicate constant intervening gaze shifts before the second-step saccade ranging from 20 degrees to the left of the primary eye position for the upper diagonal curve to 20 degrees to the right for the lowest curve in steps of 10 degrees.

These simulations use the following parameters. The intercept of the linear gain field function has been set to 1.0. The slope of the gain field function has both a linear and a small quadratic dependence on the receptive field eccentricity given by $\boldsymbol{slope} = -0.0009 * \boldsymbol{\rho} - \mathrm{sgn}(\boldsymbol{\rho}) * 2.9 \times 10^{-6} * \boldsymbol{\rho}^2$. The overall magnitude of the gain field does not affect the performance of the model as long as the ratio of slope to intercept remains the same. The receptive field size of the neurons increases with the eccentricity following the relation: $\boldsymbol{\sigma} = 30^\circ + 0.21 * \ Abs(\boldsymbol{\rho})$. The receptive field sizes are well within the range reported by Bruce and Goldberg (1985) for frontal eye field neurons (average direction tuning width = 45 degrees, average amplitude tuning = 18 degrees). A more extensive discussion of the effect of the change in receptive field size on the slope of the gain field function is given in the appendix.

Figure 3 compares the gaussian-exponential model in equations 2.3 and 2.4 to the linear rectified approximation used in the simulations. Figure 3A shows the population response to a 12 degree leftward saccade for various target locations using the gaussian-linear rectified model. The solid vertical line shows the retinal location of 12 degrees to the left of the fovea. The

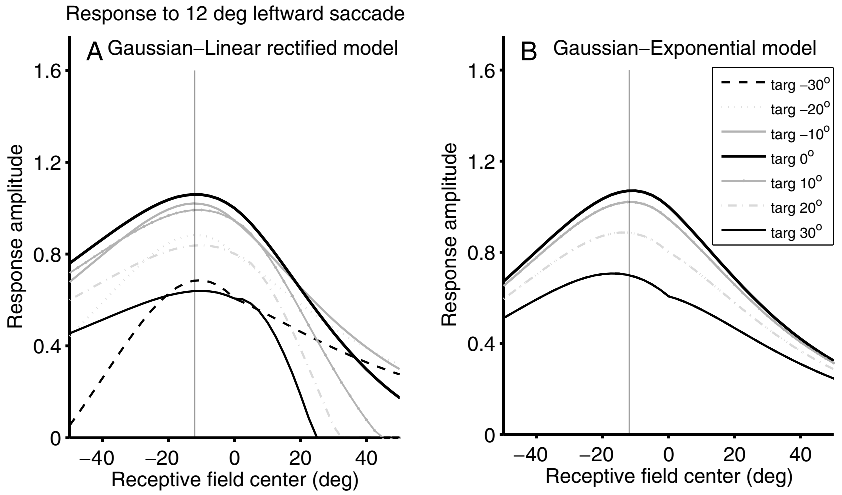

Figure 3: (A) Population tuning for a 12 degree leftward saccade (vertical line) using the gaussian-linear rectified model. The different curves represent various combinations of initial target position and eye position, all giving rise to the same saccade. (B) Population tuning for a 12 degree leftward saccade (vertical line) using a gaussian-exponential gain field model, again for various combinations of initial target position and eye position.

derivation given in the previous section predicted exponential eye sensitivity functions. Plots similar to those of Figure 3A are presented in Figure 3B for a gaussian-exponential gain field model. It is interesting that both the population response and the individual neuron selectivity for saccades (not shown) obtained with the exponential model are not as sharp as in the quasi-linear model. In addition, the response of the quasi-linear model can be driven higher for a comparable set of parameters and relatively small saccades using a gain field intercept larger than one. For the gaussian-exponential gain field model, the coefficient of the eye position term (which becomes the slope of the gain field function in the quasi-linear model) is predicted to be $-\boldsymbol{\rho}/\boldsymbol{\sigma}^2$. This condition can be relaxed in the quasi-linear model. The gaussian-linear rectified model does not require the gain field slope to be strictly equal to $-\boldsymbol{\rho}/\boldsymbol{\sigma}^2$ because there is a trade-off between the gain field slopes and intercept.

2.4 Saccade Tuning of Single Cells. The model proposed in this article is based on a retinotopic map that remains fixed as the eye moves. Saccades are updated by shifting the peak of activity within this map in coordination with the movement of the eyes. This can be understood by considering what happens at the level of single neurons. A neuron with a gaussian receptive field centered at position ρ_0 and exponential eye position sensitivity will have a firing rate given by the product of equations 2.3 and 2.4, which can be rewritten as

$$R(x, y, \rho_0) = A \bullet \exp\left[-\frac{1}{2\sigma^2} \bullet (x - y - \rho_0)^2\right] \bullet \exp\left[\frac{1}{2\sigma^2} \bullet (y^2 - 2xy)\right]. \tag{2.8}$$

The first exponential term produces a response that is maximal for saccades for which $\boldsymbol{x} - \boldsymbol{y} = \boldsymbol{\rho}_0$. The difference, $\boldsymbol{x} - \boldsymbol{y}$, is precisely the motor error of the second saccade in a double-saccade task. Hence the gain field model can be thought of as producing neurons that represent motor error. This is a consequence of enforcing the subtraction condition on equation 2.2. If we had enforced a vector addition constraint, the first exponential in equation 2.8, while still centered at $\boldsymbol{\rho}_0$, would have resulted in tuning to the head-centered coordinates of the target, $(\boldsymbol{x} + \boldsymbol{y})$, instead of saccade tuning.

The second exponential in equation 2.8 shows a dependence on eye and retinal target position. It gives an enhancement proportional to the square of the eye displacement $(\boldsymbol{y}^2)$ and a factor $(-2\boldsymbol{xy})$ that favors the response when $\boldsymbol{x}$ and $\boldsymbol{y}$ have the opposite sign, that is, when the eye moves in a direction opposite to the initial target position. Now assume we always set the saccade target to be at the retinal receptive field of the neuron so that $\boldsymbol{x} = \boldsymbol{\rho}_0$. Then the response will be

$$R(\rho_0, y, \rho_0) = A \bullet \exp\left[-y \bullet \frac{\rho_0}{\sigma^2}\right]. \tag{2.9}$$

Therefore, there will be an enhancement of the response the farther the fixation point is located with respect to the cell receptive field center. In particular, it will be highest if target and saccade start are in opposite visual hemifields. This feature of neurons from the frontal eye field (FEF) has been reported before as evidence of the presence of a gain field-like eye position modulation and in support of the hypothesis that these neurons are performing vector subtraction computations (Balan & Ferrera, 2003).

2.5 Eye Movement–Induced Shift of the Neuronal Receptive Fields. There exists an alternative approximation to derive the form of the gain field. The solution turns out to be identical to the solution to the differential equation (see equation 2.2) if only a quasi-linear (half-rectified) term in eye displacement is considered. The approximation consists in truncating the expansion of the shift operator of Fourier analysis to the first-order term followed by a half-rectification. Gaussian receptive fields belong to a class of functions that admit a series representation written as a linear superposition of a basis set given by the family of complex exponentials. In fact, almost any spatially tuned and reasonably localized (bell-shaped) receptive field function would belong to this functional class. If its center is given by $\boldsymbol{\rho}$, the receptive field can be written in a Fourier decomposition involving the functions $\exp(i \bullet k \cdot \rho)$:

$$f(x, \rho) = A \bullet \exp\left[-\frac{1}{2\sigma^2}(x-\rho)^2\right] = \int h(x, k) \cdot \exp(i \bullet k \cdot \rho) \cdot dk. \tag{2.10}$$

The explicit form of the function h is not necessary; $\boldsymbol{k}$ is related to the spatial frequency, and only the complex exponential depends on $\boldsymbol{\rho}$ on the right-hand side.

In order to shift the underlying retinotopic map to which the coordinate $\boldsymbol{\rho}$ belongs due to an eye movement of amplitude $\boldsymbol{y}$, it suffices to shift the argument in the complex exponentials. This can be done using the following operator:

$$\exp\left[y \bullet \frac{\partial}{\partial \rho}\right] \equiv \sum_n \frac{1}{n!}\, y^n \frac{\partial^n}{\partial \rho^n},$$

since

$$\begin{aligned}\exp\left[y \bullet \frac{\partial}{\partial \rho}\right] \exp(i \bullet k \cdot \rho) &= \exp(i \bullet k \cdot \rho) \sum_n \frac{1}{n!} y^n (i \bullet k)^n \\ &= \exp[i \bullet k \cdot (\rho + y)].\end{aligned}$$

When we apply this operator to a gaussian, we get:

$$\begin{aligned} f(x, \rho) &= A \bullet \exp\left[-\frac{1}{2\sigma^2}(x-\rho)^2\right] \\ \exp\left(y \frac{\partial}{\partial \rho}\right) f &= \sum_n \frac{1}{n!} y^n \frac{\partial^n}{\partial \rho^n} f \cong \left\{1 + y \frac{\partial}{\partial \rho} + \frac{1}{2!} y^2 \frac{\partial^2}{\partial \rho^2} + \cdots \right\} f \\ &= A \bullet \exp\left[-\frac{1}{2\sigma^2}(x-\rho)^2\right] \left\{1 - \frac{\rho}{\boldsymbol{\sigma}^2} y - \frac{1}{2\sigma^2}\left(y^2 - 2xy\right) \right. \\ &\quad \left. + \frac{y^2}{2\sigma^4}(x-\rho)^2 + \cdots \right\}. \end{aligned}$$

The expression in braces contains the first terms of the expansion of the function $\exp\left(-\frac{\rho}{\sigma^2} y\right) \bullet \exp\left(-\frac{1}{2\sigma^2}\left(y^2 - 2xy\right)\right)$. These are the factors that result when we shift the gaussian receptive field by an amount $\boldsymbol{y}$. The solution must be half-waved rectified to avoid negative firing rates.

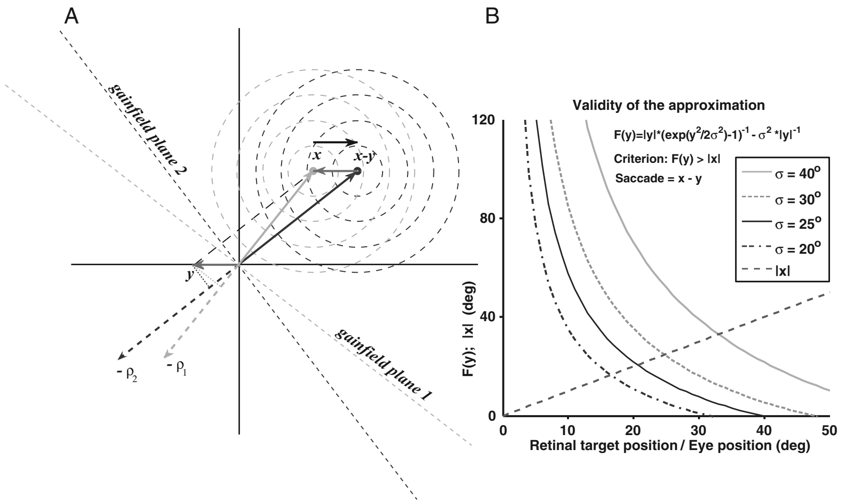

Figure 4: (A) A two-dimensional eye translation of vector $\boldsymbol{y}$ induces a shift on the retinal map origin so that the peak of activity will shift from retinotopic map location $\boldsymbol{x}$ when the target is flashed to retinotopic location $\boldsymbol{x} - \boldsymbol{y}$ right before the second step saccade. This new location of the peak of activity is the same as if the target were flashed again after the gaze shift. (B) The approximation used in this article will work as long as the values of retinal target location and eye displacement remain below the intersection point between the straight dashed line representing $F(y) > |\boldsymbol{x}|$ and the curves representing $F(y)$ for different values of sigma. Each curve corresponds to a different size of the neuronal receptive fields (see text and appendix for discussion).

This operator will always generate a first-order term linear in the shift parameter $\boldsymbol{y}$. A quadratic dependence of the receptive field shape on the eccentricity $\boldsymbol{\rho}$ will generate a linear dependence of the slope of the gain field on the eccentricity. However, the parameters should remain in the domain in which the approximation is valid. This operator can be generalized to two dimensions using a scalar product of the eye displacement and the gradient operator on the receptive field center map.

This approximation is not the same used to obtain equation 2.2. The rationales for both approximations are quite distinct. In the first case, a closed differential equation for $\boldsymbol{g}$ was derived, requiring that the population response be unimodal and enforcing the vector subtraction condition. In the second case, the shift operator quantifies the changes in the neuronal responses due to the shift of the origin of the retinotopic map—how the entire sensory field is updated by the movement of the eyes. The coincidence between both approximations implies that saccade updating and sensory field remapping are consistent.

2.6 How and Where Does the Quasi-Linear (Half-Rectified) Approximation Work? The model works by shifting the peak of activity from the retinal location given by the position of the target when flashed to a new locus at the retinal location corresponding to the required saccade. Figure 4A shows such shift from the location of the target $\boldsymbol{x}$ (where there will be a neuron with receptive field $\boldsymbol{\rho}_1$) in the retinal map when the eyes are at the fixation point before the gaze shift, to $\boldsymbol{x} - \boldsymbol{y}$ (neuron with retinal receptive field $\boldsymbol{\rho}_2$). After the gaze shift and before the second saccade, each of these neurons is modulated by a planar rectified gain field whose slope is negatively proportional to their eccentricities. In Figure 4A, the gray circles indicate the pattern of activity based on the position of the target before the gaze shift. The black circles show the pattern of activity after gaze shifts to position $\boldsymbol{y}$. In the absence of further visual stimulus, the effect of the gain fields is to shift the locus of activity to the neighborhood of $\boldsymbol{x} - \boldsymbol{y}$ in the retinotopic map. In other words, the most active cell after the gaze shift in darkness is the same cell that would have been most responsive if the eyes had moved first and the target were subsequently turned on at the same spatial location without any gain field present. For the gaussian-linear rectified model using receptive fields with uniform amplitude and size, the activities at both locations (FP1 and FP2) are

$$R_1 = A \bullet \left(1 - \frac{\vec{x} \bullet \vec{y}}{\sigma^2}\right) \quad \text{and}$$

$$R_2 = A \bullet \exp\left(-\frac{y^2}{2\sigma^2}\right) \bullet \left(1 - \frac{\overrightarrow{(x-y)} \bullet \vec{y}}{\sigma^2}\right). \tag{2.11}$$

These formulas give the responses at retinal locations 1 and 2 after the eyes have moved to the new fixation point but before the final saccade to the target. To update the metric for the final saccade to the target requires that R_2 surpasses R_1 after the gaze shift and before the final saccade to the memorized position of the target. The range within which the linear rectified model is valid is shown in Figure 4B for four different values of the receptive field size. It requires that the absolute values of retinal target position and eye displacement remain below the point of intersection of the straight line ($|\boldsymbol{x}|$) and the curves ($\mathrm{F}(\boldsymbol{y})$) in Figure 4B. A derivation of the validity condition is given in the appendix.

3 Extensions of the Basic Model

3.1 Multistep Saccades. The model can account for multistep gaze shifts in darkness because the exponential function maps multiplicative factors into addition of their arguments. Therefore, the successive application of the multiplicative modulation, first by an eye shift $\boldsymbol{y}$ followed by a shift $\boldsymbol{z}$, will result in a global multiplicative modulation dependent on the total shift $\boldsymbol{y} + z$. In the same way a product of two linear-rectified factors $(1 - \boldsymbol{y}\rho/\sigma^2) \cdot (1 - z\rho/\sigma^2)$ will approximate $(1 - (\boldsymbol{y} + z)\rho/\sigma^2 + \cdots)$.

Suppose that instead of one flash and two eye displacements in the dark, there are two successive flashes at different locations. After the first target is foveated, the model will correctly provide the updated metric for a subsequent saccade to the second flash. The order in which these saccades take place represents a decision that should be added to the model by extra variables. The model does not require the use of a temporal queue to solve this sequence of saccades.

3.2 Eye Movements in Two Dimensions. The model can be readily extended to two dimensions. In this case, the shape and orientation of the receptive field become important. Assume that the receptive field of a cell is a two-dimensional gaussian with principal variances $\boldsymbol{\sigma}_1$ and $\boldsymbol{\sigma}_2$ along the corresponding principal axes. The principal axis with the largest variance forms an angle $\boldsymbol{\theta}$ with the x-axis in a fixed (spatial) frame of coordinates, which instantaneously coincides with the retinal coordinates.

As before, $\boldsymbol{x}$ is the position vector for the saccade target, and ρ is the center of the neuron's receptive field assumed gaussian and with principal directions 1 and 2. These vectors can be represented in polar coordinates by their size and their angle with respect to the horizontal axis: $x_1 = x \cdot \cos(\alpha)$, $x_2 = x \cdot \sin(\alpha)$, $\rho_1 = \rho \cdot \cos(\beta)$, and $\rho_2 = \rho \cdot \sin(\beta)$. Substituting these in the equation above,

$$\begin{aligned} &-\frac{1}{2\sigma_1^2}(x \cdot \cos(\alpha - \theta) - \rho \cdot \cos(\beta - \theta))^2 \\ &-\frac{1}{2\sigma_2^2}(x \cdot \sin(\alpha - \theta) - \rho \cdot \sin(\beta - \theta))^2 \equiv E(x, \rho, \alpha, \beta, \theta, \sigma_{1,2}). \end{aligned}$$

The intuitive interpretation of this expression is that both vectors $\boldsymbol{x}$ and $\boldsymbol{\rho}$ are projected onto the principal axes of the receptive field. If we apply the two-dimensional version of the shift operator to the two-dimensional gaussian, we have

$$\begin{aligned} &\left\{1 + y_1 \cdot \frac{\partial}{\partial_{\rho_1}} + y_2 \cdot \frac{\partial}{\partial_{\rho_2}} + \cdots\right\} \circ \{A_1 \cdot \exp[-E\,(x, \rho, \alpha, \beta, \theta, \sigma_{1,2})]\} \\ &= A_1 \cdot \exp[-E] \bullet \{1 - y \cdot \rho \cdot [A \cdot \cos(\beta - \gamma) + B \cdot \cos(\beta + \gamma - 2\theta)] + \cdots\}. \end{aligned} \tag{3.1}$$

Here

$$A = \frac{1}{2}\left(\frac{1}{\sigma_1^2} + \frac{1}{\sigma_2^2}\right), \quad B = \frac{1}{2}\left(\frac{1}{\sigma_1^2} - \frac{1}{\sigma_2^2}\right)$$

and the eye displacement vector is given by $\vec{y} = (y \cdot \cos(\gamma)\ , y \sin(\gamma))$. The first term gives the projection of the eye displacement onto the receptive field center vector weighted by the geometric mean of the principal variances. This is an isotropic term and has no information about the shape of the receptive field. It accounts for the contributions in the direction collinear with the receptive field center. The second term measures the discrepancies between the receptive field orientation and the orientations of the receptive field center and the eye displacement. The one-dimensional case is recovered when $\gamma = \beta = \theta$ and $\gamma = \theta,\ \beta = \theta \pm \pi$. The contribution from $\boldsymbol{\sigma}_2$ cancels out, and the one-dimensional scenario applies along the direction of the receptive field eccentricity.

For circularly symmetric receptive fields, $\mathbf{B} = 0$ and $\mathbf{A} = 1/\boldsymbol{\sigma}^2$. Figure 5 shows the receptive and gain fields of two neurons in two dimensions. The slope of the planar rectified gain field is negatively proportional to the eccentricity of the receptive field center. Figure 6 shows the simulation of a two-dimensional model using circularly symmetric receptive fields. Figure 6A shows the intended eye movement. A target is flashed at position **A**, and there is an intervening gaze shift to position **B** before the final movement to the remembered target location. Figure 6B shows the population response to a single-step saccade from the center of gaze to position **A.** Figures 6C and 6D show the population activity before the first and second saccade, respectively. Figure 6D shows the population encoding of the correct second saccade vector computed as the difference between vectors **A** and **B**.

Figure 7A shows plots of the gain field slope given by the coefficient of the eye displacement $\boldsymbol{y}$ in equation 3.1 for cells with elliptical receptive field oriented at an angle $\boldsymbol{\theta}$ with respect to the horizontal axis. This direction need not be the same as the vector pointing to the center of the receptive field ($\boldsymbol{\beta}$, taken to be zero in Figure 7A). Even when the eye movement is aligned with the direction $\boldsymbol{\beta}$, equation 3.1 shows that the slope of the gain field can be changed by the effect of the receptive field orientation. In fact, the slope of the gain field may be changed smoothly between the values required for subtractive and summation conditions by appropriately tuning the orientation and aspect ratio of the neuronal receptive fields and appropriately weighting the symmetric and asymmetric contributions that enter equation 3.1. In particular, there may exist subpopulations of neurons with eye position sensitivities positively correlated with the receptive field eccentricity that would respond as if they were spatially rather than retinotopically tuned. These cells will do something other than computing vector subtraction; they could be summation cells or even cells compensating to get a pseudo-spatial or head-centered tuning fully built from retinal and eye position signals.

3.3 Rotations. This section addresses the case of a simple rigid rotation of the head (head tilt) around the center of gaze, without any eye displacement. These head rotations require head position signals originating from

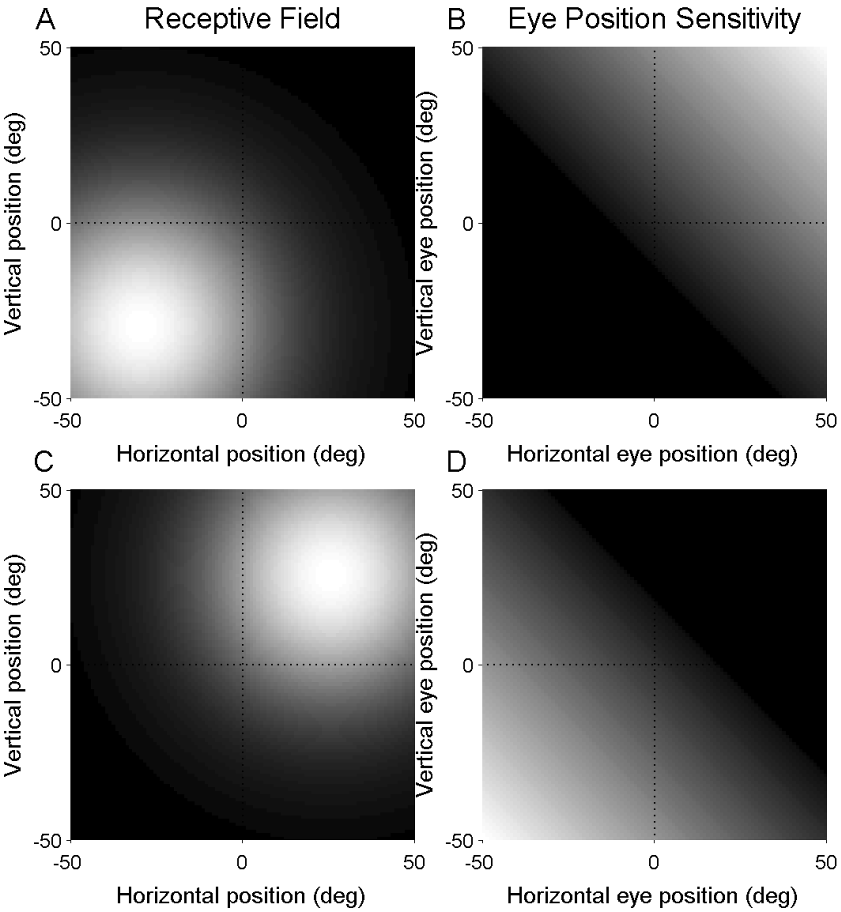

Figure 5: Example receptive fields and gain field functions in two dimensions. Firing rate is coded as gray-scale intensity level. (A) A cell with circularly symmetric receptive field centered in the lower left quadrant at (−25°, −25°). (B) The gain field function for this unit has a maximum in the upper right quadrant. (C) Unit with circularly symmetric receptive field centered in the upper right at (25°, 25°). (D) The gain field function now increases along the (−1, −1) direction.

the vestibular system rather than eye position signals. We do not address torsional movements of the eyes or the issue of noncommutativity of rigid body rotations when eye orientation is taken into account (Crawford & Guitton, 1997; Crewford, Medendorp, & Marotla, 2004; Henriques, Klier, Smith, Lowy, & Crawford, 1998; Klier & Crawford, 1998; Misslisch, Tweed, & Vilis, 1998; Smith & Crawford, 2001; Tweed, 1997; Tweed, Haslwanter, &

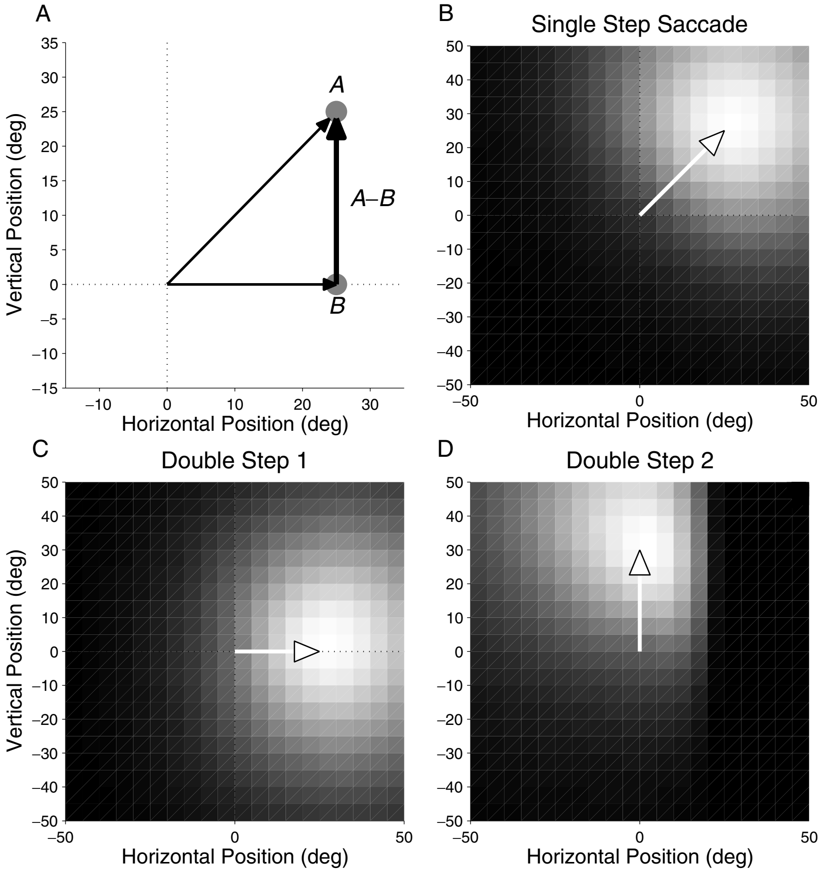

Figure 6: Saccade updating in two dimensions. (A) Eye movement from the origin in point A in one- or two-step saccades. (B) Population activity for a single-step saccade to position A in panel *A*. (C, D) A double step saccade with the same end point as in panel *B*. (C) Step 1 shows the population activity before the first saccade to the intermediate gaze position (vector B in panel *A*). Step 2 shows the updated population activity changes encoding the correct saccade vector **A-B** as shown in panel *A* has been activated by the first eye displacement.

Fetter, 1998; Medendorp, Smith, Tweed, & Crawford, 2002; see also Quala & Opticon, 1998). However, we show that a subpopulation of neurons with planar gain fields negatively correlated with their receptive field eccentricity can compensate for the visual effects of a rigid head rotation. This is at least in part consistent with the rotational remapping discussed by Medendorp et al. (2002), although we address only the simplest case without dealing with errors that accumulate across multiple saccades.

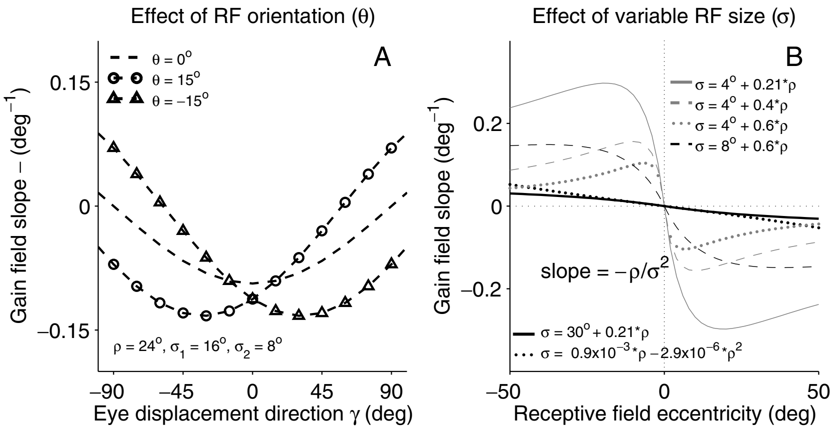

Figure 7: (A) Slope of the gain field function in two dimensions (see equation 3.1) as a function of the angle between the eye displacement (γ) and the receptive field direction (β), here taken to be horizontal (0°). The principal direction of the largest variance has an angle $\boldsymbol{\theta}$ with respect to the horizontal axis (see Figures 8A and 8B). The tilt of the receptive field with respect to the radial direction is given by $|\boldsymbol{\beta} - \boldsymbol{\theta}|$. (B) Gain field slope versus RF eccentricity for various dependences of the receptive field (RF) size $\boldsymbol{\sigma}$ on the eccentricity $\boldsymbol{\rho}$ (see the appendix for a discussion). Slopes were computed using the theoretical prediction $-\boldsymbol{\rho}/\boldsymbol{\sigma}^2$. The solid black curve uses the parameters of the simulations without further correction. The dotted black curve shows the slopes for the simulations of Figure 2.

By comparing the responses before and after the rotation, one obtains an estimate of the form of the extra retinal signals required if the process takes place in the absence of visual stimulus. A visual target is flashed at a location described by a vector of size x and angle $\boldsymbol{\alpha}$ with respect to the horizontal axis and elicits a response from a neuron with receptive field center described by a vector of eccentricity $\boldsymbol{\rho}$ and direction $\boldsymbol{\beta}$. Finally, the cell receptive field itself has an orientation with respect to the horizontal axis given by $\boldsymbol{\theta}$ (see Figures 8A and 8B).

Using the parameterization we developed in the previous section, we can write the visual response of our generic neuron as

$$R(0) = A \exp\left\{-\frac{1}{2\sigma_1^2}\left[x\cos(\alpha-\theta) - \rho\cos(\beta-\theta)\right]^2 - \frac{1}{2\sigma_2^2}\left[x\sin(\alpha-\theta) - \rho\sin(\beta-\theta)\right]^2\right\}.$$

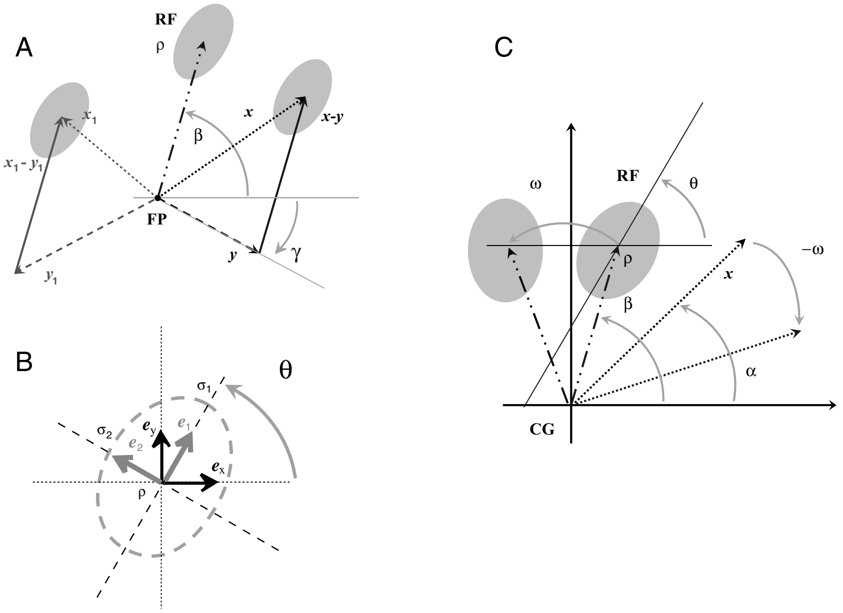

Figure 8: (A) Effect of gaze shifts for two different configurations of target $\boldsymbol{x}$ and eye displacement $\boldsymbol{y}$. The cell with receptive field $\boldsymbol{\rho} = \boldsymbol{x} - \boldsymbol{y} = \boldsymbol{x}_1 - \boldsymbol{y}_1$ will give the correct updating for arbitrary values of $\boldsymbol{x}$ and $\boldsymbol{y}$ as long as the difference remains congruent with its RF because its RF will always land on the remembered target location. This is also independent of the FP location. γ is the direction of the eye displacement vector. β is the direction of the RF in the retinal map. (B) Receptive field with orientation θ with respect to the horizontal axis in two dimensions. Black arrows indicate the unit vectors in the canonical directions. Gray arrows show the corresponding vectors along the principal directions of the RF. (C) Effect of a (head) counterclockwise rotation around the CG by an angle $\boldsymbol{\omega}$. The neuron with RF vector center given by $\boldsymbol{\rho}$ and $\boldsymbol{\beta}$, shifts to a new orientation given by $\boldsymbol{\beta} + \boldsymbol{\omega}$ with the same eccentricity. The target position vector $\boldsymbol{x}$ with orientation $\boldsymbol{\alpha}$ stays fixed in space, so that when viewed from the retinal map reference frame, it appears as if it has been rotated clockwise or by an angle $-\boldsymbol{\omega}$. The neuron's RF is assumed to be a gaussian with principal axis oriented at an angle $\boldsymbol{\theta}$ with respect to the horizontal axis. This angle need not be aligned with the RF vector direction.

$\alpha - \theta$ and $\beta - \theta$ are, respectively, the angles between the directions of the vectors $\boldsymbol{x}$ and $\boldsymbol{\rho}$ and the first principal axis of the receptive field. Thus, this expression describes the projections of these vectors onto the cell's receptive field.

When the head rotates around the center of gaze by an angle ω, it induces a rotation on the retinal map. From the reference frame of a single neuron whose receptive field moves with the map, this operation is equivalent to a rotation of the vector $\boldsymbol{x}$ in the opposite direction, changing the angle $\boldsymbol{\alpha}$ to $\boldsymbol{\alpha} - \boldsymbol{\omega}$:

$$R(\omega) = A \exp\left\{-\frac{1}{2\sigma_1^2}[x\cos(\alpha - \omega - \theta) - \rho\cos(\beta - \theta)]^2 - \frac{1}{2\sigma_2^2}[x\sin(\alpha - \omega - \theta) - \rho\sin(\beta - \theta)]^2\right\}.$$

The cross terms involving ρ and x that arise solely due to the rotation are

$$\begin{aligned} R(\omega) \approx A \cdot f(\omega = 0) \bullet \exp\Big\{2x^2\boldsymbol{B}\Big[\sin^2\left(\frac{\omega}{2}\right)\cos\Big[2\left(\alpha - \theta - \frac{\omega}{2}\right)\Big] \\ - \sin\left(\frac{\omega}{2}\right)\sin\left(2(\alpha - \theta) - \frac{\omega}{2}\right)\Big]\Big\} \\ \bullet \exp\Big\{2x\rho\sin\left(\frac{\omega}{2}\right)\Big[\boldsymbol{A}\sin\left(\alpha - \beta - \frac{\omega}{2}\right) \\ + \boldsymbol{B}\sin\left(\alpha + \beta - 2\theta - \frac{\omega}{2}\right)\Big]\Big\}. \end{aligned}$$

If the receptive field is reasonably round so that $\boldsymbol{\sigma}_1 \sim \boldsymbol{\sigma}_2$, then $\boldsymbol{A}$ approximates $\mathbf{1}/\boldsymbol{\sigma}^2$ and $\boldsymbol{B} \sim 0$. In this case, the equation, up to linear terms, simplifies to

$$R(\omega) \approx A \cdot f(\omega = 0) \bullet \left\{1 + 2\frac{x\rho}{\sigma^2}\sin\left(\frac{\omega}{2}\right)\sin\left(\alpha - \beta - \frac{\omega}{2}\right) + \cdots\right\}.$$

For simplicity, assume that the target flashes on the horizontal axis in the right visual hemifield, and consider small counterclockwise rotations. Then $\boldsymbol{\alpha} = 0$ and $\boldsymbol{\omega} > 0$ but small so that $\sin\left(\frac{\omega}{2}\right) \approx \frac{\omega}{2}$, and we can further neglect $\frac{\omega}{2}$ when compared with $\boldsymbol{\beta}$. The gain field then reads

$$g(x, \rho, \beta, \omega) = g_0 \bullet \left(1 - x\omega \cdot \frac{\rho}{\sigma^2} \cdot \sin(\beta) + \cdots\right).$$

The extraretinal signal is provided by $\boldsymbol{x}\omega$, which plays a similar role to the eye displacement in the case of translations. It ($\boldsymbol{x}\omega$) is indeed the information about the shift of the target location over the retinal map that must be supplied by extraretinal signals if the head rotation occurs in the dark. The factor $\sin(\beta)$ will have its maximum value of 1 at $\beta = \frac{\pi}{2} = 90^\circ$, which is perpendicular to the direction of the target position vector. Hence, neurons with receptive field center along the positive vertical axis will have a maximal negative slope in their gain fields. This suggests that the circuitry implementing the gain field modulation for translations would

Table 1: Saccade Error versus Neuronal Pool Size.

n	A	Error (deg)
1	25	5.89
10	25	3.64
100	25	2.67
1000	25	3.13
1	100	5.32
10	100	2.68
100	100	1.74
1000	100	1.43

also work for this type of rotations. The only difference is that the rotation signal should be fed—presumably from a different extraretinal source—into the neurons with receptive field vector aligned perpendicular to the target position vector.

3.4 Effect of Noise on Model Performance. To address the probabilistic nature of the neuronal responses, we run simulations of the model with Poisson distributed noise in the output. We considered each node in the model to represent a pool of neurons, all having the same receptive field and eye position sensitivity. The response of each node is given by

$$r\,(x, y) = \text{median}\,[\text{Poisson}\,(n, A * f\,(x) * g\,(y))]\,,$$

where $r(x, y)$ is the response as a function of retinal target location (x) and eye position (y); n is the number of cells in the pool; A is a constant that determines the average firing rate and is the same for all nodes; and $f(x)$ and $g(y)$ are the underlying retinal and eye position sensitivities. The function "Poisson" generates n Poisson-distributed random deviates with $\lambda = A * f(x) * g(y)$. The response of the node is computed by taking the median of this sample.

In a range of saccade amplitudes between −60 and 60 degrees the performance depends on the overall firing rate (A) and the pool size (n). Table 1 shows average saccade error for $A = 25$ or 100 spikes per second and neuronal pool sizes (n) from 1 to 1000. Thus, with n larger than 10 and firing rates over 25 spikes per second, the average error remains around or below 3 deg, which represents a typical spread in saccade end points in stimulation experiments of the FEF (Bruce & Goldberg, 1985).

4 Discussion

In a population of neurons with tuned retinal receptive fields that are modulated multiplicatively by eye position–dependent gain fields, vector subtraction can be computed by shifting the peak of the population activity in a retinotopic map provided that there is a systematic relationship between the parameters of the retinal and eye position sensitivity functions. The vector subtraction computation and the requirement of response unimodality impose constraints on this relationship across the neuronal population. Specifically, the slope of the eye position sensitivity should be negatively proportional to the receptive field eccentricity. This computation generalizes to any system with cells in which one input is encoded in a topographic map and the other input follows a rate code proportional to the displacement of the center of that map. We have applied this general idea to the specific case of double-step saccades in the FEF. We have shown how this sensory and eye displacement integration gives origin to a topographic organization of saccade vectors preference independent of the initial gaze direction, in accordance with results from microstimulation experiments (Robinson & Fuchs, 1969; Mushiake, Tanatsugu, & Tanji, 1997; Mushiake, Fujii, & Tanji, 1999; Russo & Bruce, 1993). We supported the theoretical derivations with simulations in one and two dimensions using units with gaussian receptive fields and linear-rectified eye position–dependent gain fields.

Neuronal responses can be tailored to compensate to various degrees for the eye movement–induced displacement of their receptive fields by adjusting the slope of the eye position dependence of the multiplicative modulation. In the model described here, all receptive fields are retinal. They do not shift or change form. The eye position modulation is exclusively an amplitude modulation. In this sense, this model is parsimonious. It does not invoke shifting receptive fields or intermediate encoding stages or representations. Plasticity in the shape and orientation of the receptive field could allow recruitment of neurons to encode saccade in a given direction.

4.1 Relation to Previous Work.

4.1.1 Neural Network Approaches. Xing and Anderson (2000), elaborating on previous work by Zipser and Andersen (1988), implemented a neural network that could keep memory of the position of subsequent targets and was able to perform a double-step saccade. Their model was explicitly intended to reproduce the behavior of neurons from the lateral parietal area (LIP). Their network stored a queue of the various target representations and maintained the memory of them in neuronal delayed activity until the saccade was executed. The analysis of the hidden units of the network showed that the cells developed very large receptive fields and that their responses could be represented using multiplicative gain fields with a planar dependence on eye position. Interestingly, the hidden unit population splits into two subgroups. Type I units encode the location of the target in head-centered coordinates by computing the addition of the target retinal representation vector and the eye position vector. These units display a planar rectified gain field encoding the eye position that ramps up in the same direction as the retinal receptive field of the unit. Type II units encode the desired saccade vector to the second target. They also display a planar rectified gain field encoding the eye position, but in this case the planar function ramps up opposite to the prefered location of their visual receptive field. Our model suggests how cells with those characteristics can perform the computations of vector addition and subtraction and how it is related to the slope of the gain field function encoding the eye position.

Salinas and Abbott (1995) have shown very generally how to use gain fields to compute virtually any kind of linear transformation downstream from the neurons on which the information about retinal location and eye position converges. These authors used linear-rectified gain fields with positive and negative slopes for the eye position coefficient. A difference between their model and the one presented here is that their gain fields have preferred gaze locations distributed uniformly across the eye position domain. Their model requires a translational invariant encoding of the eye position input. In our model, this requirement is absent, as the only preferred gaze location is the center of gaze. Salinas and Abbott (1996) have also shown how to obtain multiplicative responses out of additive inputs by virtue of the use of recurrent connections in a network of neurons. We shall not discuss this point further here since our starting point already assumes multiplicative gain fields. However, our results are consistent in principle with their results.

Pouget and Sejnowski (1997) and Pouget, Fisher, and Sejnowski (1993) suggested that neurons in the parietal cortex may display responses given by products of gaussians representing retinal position and sigmoids that encode eye position. A set of functions constructed in that way constitutes a basis of their functional space so that any function of those variables can be written as a linear superposition of the elements of the basis. They also pointed out that linear rectified functions of eye position can replace the sigmoids since the saturation at zero provides the required nonlinearity.

A significant difference between our model and that of Pouget and Sejnowski (1997) is that the latter used a family of sigmoids with constant eye position coefficient and inflexion points uniformly spaced across the eye position domain. While the encoding of any nonlinear function of retinal and eye positions is guaranteed, the lack of a systematic dependence on the (oculocentric) topography of the population of neurons results in encoding through a distribution of learnable weights across the members of the basis functions and the need of a population average readout stage downstream. In our model, each unit is already able to respond maximally across the map when the saccade metric congruent with its retinotopic field is required. There is no weight learning required, although it is not precluded, and the saccade updating can be read from the peak activity location.

The model presented here uses the eye displacement with respect to the instantaneous center of gaze, which is not equivalent to other points in the eye position field. Encoding of the eye position in a translational invariance manner is therefore not explicitly required, and although not precluded, there is no need for a representation of the orbital position of the eye or direction of gaze.

Quaia and collaborators (Quaia et al., 1998) addressed the computation of vector subtraction in the FEF using switching circuits. Their model was intended to predict the saccade vector for the second saccade of a double-saccade task. They constructed a neural network with units that resemble responses of neurons from area LIP and FEF that is able to perform this calculation. Their main premise is that the brain does not require an explicit supraretinal representation of the target given, for example, in external space or body-centered coordinates. Instead it suffices to buffer information in the tonic and sustained activity of neurons in areas LIP and FEF in order to obtain a dynamic remapping of the visual space.

4.1.2 Analytic Approaches. Siegel (1998) addressed a similar question in relation to neurons from area 7a and showed how to use a population average encoding strategy, the center-of-mass equation, to decode the position of an object in head-centered coordinates, knowing its retinal representation and the eye position. This computation is a weighted average of the retinal locations using as a weight the eye position gain field. In order to link the two factors, one needs to assume a dependence of the gain field parameters on the receptive field location of the cell encoding the retinal location of the target. Seigel showed that it is possible to encode linearly the head-centered coordinates of the object assuming that the responses of the neurons of area 7a are modulated by a gain field that is linear in the eye position and assuming that the intercept parameter of such gain field function varies linearly proportional to the location of the center of the receptive field of the cell.

4.2 Relation to Behavioral Tasks and Electrophysiological Experiments. A necessary condition for this model to work is the presence of appropriate eye position signals in the FEF. We report on the experimental quantification of these signals in a separate work (Cassanello & Ferrera, 2005). This modulation would allow the cell population to predict the new position of the target with respect to the displaced retinal map. This change in response could be anticipatory to a saccade (efference copy) and provide the correct metric for the desired eye movement (Colby, Duhamel, & Goldberg, 1996; Duhamel, Colby, & Goldbergm 1992; Golberg & Bruce, 1990; Umeno & Goldberg, 1997; Walker, Fitzgibbon, & Goldberg, 1995). Alternatively, it could be an afferent signal from extraocular proprioceptors. In an electrophysiological experiment, if the fixation point is eccentric to the center of gaze, the background activity or the response to a peripheral visual target should reveal the afferent signal. If this circuitry is hard-wired in the neuronal population, a task consisting of visually guided saccades with starting points at various eccentric locations along the preferred direction of a cell's receptive field should be able to uncover the negative correlation between receptive field eccentricity and slope of the eye position gain field (e.g., Andersen et al., 1990).

The model predicts a correlation between the value of the slope of the eye position sensitivity function and the ratio between receptive field eccentricity and the square of the receptive field size ($\boldsymbol{\rho}/\boldsymbol{\sigma}^2$). That correlation is an identity in the case of the exponential gain field and gets relaxed in the linear-rectified model. It will also be affected by variation of the receptive field size with eccentricity and by the presence of background firing (see the appendix). The model presented here can be enriched by adding further dependencies on other variables such as eye velocity or acceleration or more complicated dynamics.

5 Conclusion

Eye position signals that modulate visual activity have proven to be pervasive across several areas of the brain like LIP, 7a, V4, and superior colliculus (Andersen et al., 1985; Andersen et al., 1990; Siegel, 1998; Salinas & Abbott, 1995; Bremmer, Ilg, Thiele, Distler, & Hoffmann, 1997; Bremmer, Pouget, & Hoffmann, 1998; DeSouza et al., 2000; Funahashi & Takeda, 2002; Xing and Andersen, 2000; Snyder, 2000; Van Opstal et al., 1995; Campos et al., 2006), and there is plenty of evidence from neurophysiogical data from the FEF (Cassanello & Ferrera, 2005). The idea of gain field modulations taking place in several areas of the brain is not new, nor is the proposal of using linear rectified gain fields. However, to the best of our knowledge, this algorithm and the rationale used to derive it have not been presented before. In our opinion this work complements and illuminates approaches based on neural networks.

The general algorithm can be applied to maps in other areas of the brain and of other features (e.g., an auditory map), which can be integrated with position signals from different areas of the brain known to encode such signals. The gain field modulation, appropriately tuned, can implement coordinate transformations into various frames of reference and produce neuronal responses that may look retinotopically tuned, head-centered tuned, or intermediate between these limits. This may explain intermediate coordinate frames found in studies of foveating or reaching for objects (Mullette-Gillman, Cohen, & Groh, 2005; Baker, Harper, & Snyder, 2003; Batista, Buneo, Snyder, & Andersen, 1999; Buneo, Jarvis, Batista, & Andersen, 2002). This property gives a large flexibility to the algorithm, and because of the simplicity of its implementation, it may well be the computational tool of choice for the brain. What has to be tailored is the way in which the different extraretinal signals that one wants to integrate with the visual ones get fed. However, this is just a matter of choosing the correct circuitry at the level of the inputs. The planar slope in the relevant gain field is virtually all that is needed, and it is everywhere.

Appendix

A.1 Validity of the Linear Rectified Approximation. The shift in the peak of population activity can be understood by comparing the response elicited by a target flashed twice at the same spatial location: the first time with the eyes at FP1 and the second time after an eye displacement $\boldsymbol{y}$ to FP2 (see Figure 4A). The cell with receptive field center at position $\boldsymbol{\rho}_1 = \boldsymbol{x}$ will give a response $\boldsymbol{A}$ when the target is flashed with the eyes at FP1. The cell with receptive field at $\boldsymbol{\rho}_2 = x - y$ will give a smaller response of value $\boldsymbol{A} \cdot \exp(-\boldsymbol{y}^2/\mathbf{2}\boldsymbol{\sigma}^2)$, because their receptive field centers are separated by $\boldsymbol{y}$. When the eyes fixate at FP2 and the target is flashed at the same spatial location, cell 1 will decrease its response to $\boldsymbol{A} \cdot \exp(-\boldsymbol{y}^2/\mathbf{2}\boldsymbol{\sigma}^2)$ and cell 2 will increase its response to $\boldsymbol{A}$ since the target is now at the center of its receptive field. Our working hypothesis is that the brain mimics this switch in activity when there is no second flashing of the target. For the linear-rectified approximation, these activities are shown in equation 2.11. The regime of values of $\boldsymbol{x}$ and $\boldsymbol{y}$ in which R_2 grows higher than $R_{1,}$ and consequently the peak of activity shifts from $\boldsymbol{\rho}_1$ to $\boldsymbol{\rho}_2$, is defined by the condition:

$$\left(1 - \frac{\vec{x} \bullet \vec{y}}{\boldsymbol{\sigma}^2}\right) \leq \exp\left(-\frac{y^2}{2\boldsymbol{\sigma}^2}\right) \bullet \left(1 - \frac{\overrightarrow{(x-y)} \bullet \vec{y}}{\boldsymbol{\sigma}^2}\right),$$

which implies

$$-|x| \bullet \cos(\alpha) \leq |y| \bullet \left(\exp\left(\frac{y^2}{2\boldsymbol{\sigma}^2}\right) - 1\right)^{-1} - \frac{\boldsymbol{\sigma}^2}{|y|}.$$

Here α is the angle between the vectors $\boldsymbol{x}$ and $\boldsymbol{y}$. The most unfavorable situation occurs when these vectors point in opposite directions, or $\mathbf{cos}(\boldsymbol{\alpha}) = -1$. These are the curves plotted in Figure 4B for several values of $\boldsymbol{\sigma}$. If the eye sensitivity functions intercept at a value larger than one, the range of validity will be enhanced because the curves $\mathbf{F}(\boldsymbol{y})$ will be shifted to the right. Equivalently, the intercept can be kept at unity, reducing the gain field slope by the inverse of the intercept. The error in the correct position of $\boldsymbol{\rho}_2 = \boldsymbol{x} - \boldsymbol{y}$ can be computed by taking the derivative of equation 2.7 with $A_2 = \mathbf{1}/\boldsymbol{\sigma}^2$, at $\boldsymbol{x}$ and $\boldsymbol{y}$ fixed, finding the root of this derivative set equal to zero and comparing the value of the root to the correct saccade metric $\boldsymbol{x} - \boldsymbol{y}$.

A.2 Two-Dimensional Receptive Field Parameterization. The unit vectors along the principal axes of the cell receptive field centered at $\boldsymbol{\rho}$ can be written in terms of the unit vectors along the canonical axes (see

Figure 9B):

$$\vec{e}_1 = \cos(\theta)\,\vec{e}_x + \sin(\theta)\,\vec{e}_y$$
$$\vec{e}_1 = -\sin(\theta)\,\vec{e}_x + \cos(\theta)\,\vec{e}_y$$

so that the inverted relation is:

$$\vec{e}_x = \cos(\theta)\,\vec{e}_1 - \sin(\theta)\,\vec{e}_2$$
$$\vec{e}_y = \sin(\theta)\,\vec{e}_1 + \cos(\theta)\,\vec{e}_2.$$

A vector $\vec{\nu} = (\nu_x, \nu_y)$ can be written in the basis $\{\vec{e}_1, \vec{e}_2\}$ and the components will be

$$\vec{\nu} = \nu_x\vec{e}_x + \nu_y\vec{e}_y = (\nu_x\cos(\theta) + \nu_y\sin(\theta))\,\vec{e}_1 + \left(-\nu_x\sin(\theta) + \nu_y\cos(\theta)\right)\,\vec{e}_2.$$

If we replace the vector $\vec{\nu} = \vec{x} - \vec{\boldsymbol{\rho}} = (x_1 - \boldsymbol{\rho}_1)\,\vec{e}_x + (x_2 - \boldsymbol{\rho}_2)\,\vec{e}_y$, the argument of the gaussian representing the retinal receptive field becomes

$$-\frac{1}{2\boldsymbol{\sigma}_1^2}\left((x_1 - \boldsymbol{\rho}_1)\cos(\theta) + (x_2 - \boldsymbol{\rho}_2)\sin(\theta)\right)^2$$
$$-\frac{1}{2\boldsymbol{\sigma}_2^2}\left(-(x_1 - \boldsymbol{\rho}_1)\sin(\theta) + (x_2 - \boldsymbol{\rho}_2)\cos(\theta)\right)^2.$$

A.3 Generalization to Other Shapes of Receptive Fields. Equation 2.2 can be applied to other receptive field shapes. Examples of visual receptive fields that have the shape of unimodal localized spatial functions are:

$f(x, \rho)$	$g(y, \rho)$
$f_0 \bullet \left[1 - \left(\frac{x-\rho}{\sigma}\right)^2\right]$	$g_0 \bullet \exp\left[-2 \bullet y \bullet \left(\frac{\boldsymbol{\rho}}{\sigma^2}\right) \bullet \left(\frac{1}{1-(y/\sigma)^2}\right)\right]$ $\cong -2 \bullet y \bullet \left(\frac{\rho}{\sigma^2}\right) \bullet \left[1 + \left(\frac{y}{\sigma}\right)^2 + \cdots\right]$
$\begin{cases} f_0 \bullet \cos^n\left(\frac{\pi}{2n}(x-\rho)\right) & \text{for } \lvert x-\rho\rvert \le \sigma \\ 0 & \text{otherwise} \end{cases}$	$g_0 \bullet \exp\left[-\left(\frac{n\cdot\pi}{2\sigma}\rho\right) \bullet \tan\left(\frac{\pi}{2\sigma} \bullet y\right)\right]$ $\cong g_0\left[1 - y \bullet \left(\frac{n\cdot\pi}{2}\right)\left(\frac{\rho}{\sigma^2}\right) + \cdots\right]$
$f_0 \bullet \left(\cosh\left(\frac{x-\rho}{\sigma}\right)\right)$	$g_0 \bullet \exp\left[-\frac{\rho}{\sigma} \bullet \tanh\left(\frac{y}{\sigma}\right)\right]$ $\approx g_0 \bullet \left[1 - y \bullet \frac{\rho}{\sigma^2} + \cdots\right]$

$$\begin{aligned} & f_0 \bullet \left(\frac{1}{(x - \boldsymbol{\rho})^2 + \sigma^2} \right) && g_0 \bullet \exp \left[-2 \cdot y \cdot \frac{\boldsymbol{\rho}}{y^2 + \sigma^2} \right] \\ & = \frac{f_0}{\sigma^2} \bullet \left(1 + \left(\frac{x - \boldsymbol{\rho}}{\sigma} \right)^2 \right)^{-1} && \cong g_0 \bullet \exp \left(-2 \cdot y \cdot \frac{\boldsymbol{\rho}}{\sigma^2} \cdot \frac{1}{1 + (y/\boldsymbol{\rho})^2} \right). \end{aligned}$$

In all of these examples, the companion gain field is an exponential of a function of the eye displacement, with coefficients negatively proportional to the receptive field eccentricity and inversely proportional to the square width of the receptive field. The first-order approximations to these expressions are linear-rectified gain fields, with slopes proportional to the same combination of parameters.

A.4 Effect of Receptive Field Size. If there is a systematic dependence of the receptive field size on the receptive field eccentricity, this dependence enters equation 2.2 and affects both exact solution and linear-rectified approximation of the gain field. In particular, the gain field slope can be different from the ratio $-\boldsymbol{\rho}/\boldsymbol{\sigma}^2$.

When the receptive field $\boldsymbol{\sigma}$ depends on the eccentricity $\boldsymbol{\rho}$, equation 2.2 changes into

$$\frac{1}{\sigma^3} \frac{\partial \sigma}{\partial \rho} (x - \rho)^2 + \frac{1}{\sigma^2} (x - \rho) + \frac{\partial}{\partial \rho} \log(g) \bigg|_y = 0. \tag{A.1}$$

A simple linear dependence of the receptive field size on the eccentricity is $\sigma(\rho) = \sigma_0 (1 + \frac{\rho}{\lambda})$, so that for foveal values of ρ, the size of the receptive field is roughly $\boldsymbol{\sigma}_0$, and $\boldsymbol{\lambda}$ gives a spatial scale over which $\boldsymbol{\sigma}$ becomes proportional to the eccentricity. Figure 8B shows the region of expected values of the gain field slope for single cells, for reasonable ranges of $\boldsymbol{\sigma}_0$ and $k = \sigma_0 / \lambda = 0.4$. The equation that determines $\boldsymbol{g}$ becomes

$$\frac{\partial}{\partial \rho} \log(g) \bigg|_y = -\frac{1}{\sigma^2} (x - \rho) - \frac{1}{\sigma^3} \frac{d\sigma}{d\rho} (x - \rho)^2 = -\frac{1}{\boldsymbol{\sigma}^2} y - \frac{1}{\boldsymbol{\sigma}^3} \frac{d\sigma}{d\rho} y^2. \tag{A.2}$$

The second term on the right-hand side arises from the dependence of $\boldsymbol{\sigma}$ on $\boldsymbol{\rho}$. This term introduces a direct quadratic dependence of the slope of the gain field on the eye position. This dependence is different from the one induced by the retinal shift. It has the opposite sign, and it enters the term of the gain field that depends linearly on the receptive field eccentricity and therefore in a systematic way on the retinotopic map. When $\boldsymbol{k} = 0$, one recovers equation 2.2. Integrating equation A.2 over $\boldsymbol{\rho}$ gives the following formal expression:

$$
\begin{aligned}
\log\left(g/g_0\right) &= -y\int_{\sigma(0)}^{\sigma(\rho)} \frac{d\sigma}{\sigma^2(t)}\frac{1}{d\sigma/dt} - y^2\int_{\sigma(0)}^{\sigma(\boldsymbol{\rho})} \frac{d\sigma}{\sigma^3(t)} \\
&= -y\int_{\sigma(0)}^{\sigma(\boldsymbol{\rho})} \frac{d\sigma}{\sigma^2(t)}\frac{1}{d\sigma/dt} - \frac{1}{2}y^2\left(\frac{\sigma^2(\rho)-\sigma^2(0)}{\sigma^2(0)\,\sigma^2(\rho)}\right).
\end{aligned}
$$

If we use for $\boldsymbol{\sigma}$ the specific linear form given below equation A.1, we get

$$
\begin{aligned}
\log\left(g/g_0\right) &= -\frac{\rho}{\sigma_0\sigma}y - \frac{1}{2}y^2\frac{k\rho\left(\sigma^2-\sigma_0^2\right)}{\sigma_0^2\sigma^2} \\
&= -\frac{\rho}{\sigma_0\left(\sigma_0+k\rho\right)}y - \frac{1}{2}y^2\frac{k\rho\left(2\sigma_0+k\rho\right)}{\sigma_0^2\left(\sigma_0+k\rho\right)^2}.
\end{aligned}
$$

Notice that now the slope of the gain field function is given by$\rho\big/\sigma_0\left(\sigma_0+k\rho\right)$. There are two limits to consider here. When $\boldsymbol{\sigma}_0 \gg \boldsymbol{\rho}$, the slope of the gain field approximates the ratio ρ/σ_0^2 as when the width of the receptive field does not depend on the eccentricity. When $\boldsymbol{\sigma}_0 \ll \boldsymbol{\rho}$, the slope of the gain field is given by the ratio $(1/k\sigma_0)(1-\sigma_0/k\boldsymbol{\rho})$. The second factor is almost one because $\boldsymbol{\rho} \gg \sigma_0$. The slope becomes independent of the eccentricity and could become very flat or very steep, depending on the values of $\boldsymbol{k}$ and $\boldsymbol{\sigma}_0$.

If the size of the receptive field changes from, say, 5 to 25 degrees over a 50 degree range, then $k \approx 0.4$. Figure 7B shows plots of the value of the gain field slope versus the receptive field eccentricity for $\boldsymbol{k} = 0.21$, 0.4, and 0.6, with small foveal $\boldsymbol{\sigma}_0$. There is also a plot of the slopes obtained using the parameters of the simulations (see Figure 2) for which $\boldsymbol{\sigma}_0 = 30^\circ$ and $\boldsymbol{k} = 0.21$, and a plot of the gain field slopes including the small quadratic dependence on the receptive field eccentricity.

One can consider two other cases, one of which can be computed exactly:

1. $\sigma(\rho) = \sigma_0\exp(\rho/\lambda)$, in which case, $\boldsymbol{\sigma}$ grows faster than any power of $\boldsymbol{\rho}/\lambda$.
2. $\sigma(\rho) = \sigma_0 + \sigma_0\ln(1+\rho/e\lambda)$, where $\boldsymbol{\sigma}$ grows slower than any power of $\boldsymbol{\rho}/\boldsymbol{e\lambda}$.

Case 1 gives the solution:

$$
\log\left({}^{g}\!/_{g_0}\right) = -y\frac{\boldsymbol{\rho}}{\sigma_0^2}\left(1-\frac{\boldsymbol{\rho}}{\lambda}\right)\left[1+\frac{y}{\lambda}\right].
$$

The slope of the gain field can change dramatically depending on $\boldsymbol{\lambda}$. An intuitive interpretation for this parameter would be the scale of the foveal representation in cortex. For eccentricities below $\boldsymbol{\lambda}$, the receptive field sizes would be roughly constant. Beyond that scale, the receptive field size grows strongly with the eccentricity. If $\boldsymbol{\lambda}$ is very large, we recover the result derived before, and the slope of the gain field would be the ratio $\boldsymbol{\rho}/\boldsymbol{\sigma}^2$. Loosely speaking, this would be the case in which our entire retina is foveal. If $\boldsymbol{\lambda}$ is of the order of 5 to 10 degrees, the interesting twist is that the slope of the gain field function reverses sign beyond that eccentricity. If this were the correct scenario, the gain field slopes of neurons with very eccentric receptive fields could be positively correlated with the receptive field center. Admittedly, a rate of receptive field growth exponential on the eccentricity is extreme, but this example points out that the predicted negative correlation between gain field slopes and receptive field eccentricity should not be demanded for every neuron.

The other case can be estimated. We arrive at the following expression:

$$\log(g/g_0) = -y\frac{\lambda}{\sigma_0^2}\int_1^{\sigma(\boldsymbol{\rho})/\sigma_0} du \cdot u^{-2} \cdot \exp(u) + \frac{1}{2}\frac{y^2}{\sigma_0^2}\frac{1-\left(1+\ln\left(1+{}^{\rho}/_{e\lambda}\right)\right)^2}{\left(1+\ln\left(1+{}^{\rho}/_{e\lambda}\right)\right)^2}.$$

The integral in the first term is bounded between

$$e \cdot \ln\left(1+\frac{\rho}{e\lambda}\right) \le \int_1^{\sigma(\rho)/\sigma_0} du \cdot u^{-2} \le e \cdot \ln\left(1+\frac{\rho}{e\lambda}\right)\frac{\left(1+\frac{\rho}{e\lambda}\right)}{\left[1+\ln\left(1+{}^{\rho}/_{e\lambda}\right)\right]^2}.$$

To first order in the eccentricity $\boldsymbol{\rho}$, it is enough to use $\boldsymbol{\rho}/\lambda$ as a good estimate of this integral. When we insert this value in the previous equation, we recover the usual ratio $\boldsymbol{\rho}/\boldsymbol{\sigma}^2$ for the case of the size independent of the eccentricity. The second term, however, adds a quadratic dependence on the eye position. An estimate for the gain field slope for values of the receptive field eccentricity not significantly larger than the scale $\boldsymbol{\lambda}$ would be given by

$$\log\left({}^{g}/_{g_0}\right) = -y \cdot \frac{\rho}{\sigma_0^2} - y^2 \cdot \frac{\rho}{e\lambda\sigma_0^2} + \cdots.$$

A.5 Effect of the Background Firing Rate. The derivations presented so far neglected the presence of significant background firing in the response of the neurons. If there is background firing,

$$f(x,\rho) = A_0 + A_1 \bullet \exp\left[-\frac{1}{2\sigma^2}(x-\rho)^2\right],$$

with the same conventions used before. The derivative of the log of this function when A_0 is not negligible with respect to A_1 is

$$\frac{\partial \log[f(x.\rho)]}{\partial \rho} = \left[A_0 + A_1 \bullet \exp\left(-\frac{1}{2\sigma^2}(x-\rho)^2\right)\right]^{-1} \bullet A_1 \bullet \left(\frac{1}{\sigma^2}(x-\rho)\right) \bullet \exp\left[-\frac{1}{2\sigma^2}(x-\rho)^2\right],$$

which should be set equal to the derivative of the log of the gain field with the constraint enforced:

$$\frac{\partial \log[g(y.\rho)]}{\partial \rho} = -\left[A_0 + A_1 \bullet \exp\left(-\frac{1}{2\sigma^2}y^2\right)\right]^{-1} \bullet A_1 \bullet \left(\frac{1}{\sigma^2}y\right) \bullet \exp\left[-\frac{1}{2\sigma^2}y^2\right].$$

Integrating over $\boldsymbol{\rho}$, the gain field takes the form

$$g(y.\rho) = g_0 \bullet \exp\left[-\frac{\rho}{\sigma^2} \bullet y \bullet \left[\frac{A_1 \bullet \exp\left(-\frac{1}{2\sigma^2}y^2\right)}{A_0 + A_1 \bullet \exp\left(-\frac{1}{2\sigma^2}y^2\right)}\right]\right].$$

For $\boldsymbol{y}$ small compared to $\sqrt{2} \bullet \sigma$,

$$\frac{A_1 \bullet \left(-\frac{1}{2\sigma^2}y^2\right)}{A_0 + A_1 \bullet \left(-\frac{1}{2\sigma^2}y^2\right)} \approx \frac{A_1}{A_0 + A_1} \bullet \left[1 - \frac{A_0}{A_0 + A_1} \bullet \frac{1}{2\sigma^2} \bullet y^2 + \cdots\right]$$

and

$$g(y.\rho) \approx g_0 \bullet \exp\left[-\frac{\rho}{\sigma^2} \bullet \frac{A_1}{A_0 + A_1} \bullet y + \frac{\rho}{2(\sigma^2)^2} \frac{A_0 A_1}{(A_0 + A_1)^2} \bullet y^3 + \cdots\right].$$

The ratio $\frac{A_1}{A_0+A_1}$ reduces the size of the slope of the gain field if A_0 becomes a sizable proportion of A_1. There is also a competition between the linear and a third-order term in the eye displacement which we shall not discuss further.

Acknowledgments

This research was supported by grant NIMH MH59244. We are indebted to Lawrence Abbott for pointing out important differences between gain field models and for encouraging and enlightening suggestions. C.R.C.

thanks Ning Quian and Suresh Krishna for interesting suggestions and illuminating discussions.

References

Andersen, R. A., Bracewell, R. M., Barash, S., Gnadt, J. W., & Fogassi, L. (1990). Eye position effects on visual, memory and saccade-related activity in areas LIP and 7a of macaque. *Journal of Neuroscience, 10*(4), 1176–1196.

Andersen, R. A., Essick, G. K., & Siegel, R. M. (1985). Encoding of spatial location by posterior parietal neurons. *Science, 230*, 456–458.

Andersen, R. A., & Mountcastle, V. B. (1983). The influence of the angle of gaze upon the excitability of the light-sensitive neurons of the posterior parietal cortex. *Journal of Neuroscience, 3*, 532–548.

Baker, J. T., Harper, T. M., & Snyder, L. H. (2003). Spatial memory following shifts of gaze: Saccades to memorized world-fixed and gaze-fixed targets. *Journal of Neurophysiology, 89*, 2564–2576.

Balan, P. F., & Ferrera, V. P. (2003). Effects of gaze shifts on maintenance of spatial memory in macaque frontal eye field. *Journal of Neuroscience, 23*, 5446–5454.

Batista, A. P., Buneo, C. A., Snyder, L. H., & Andersen, R. A. (1999). Reach plans in eye-centered coordinates. *Science, 285*, 257–260.

Bremmer, F., Ilg, U. J., Thiele, A., Distler, C., & Hoffmann, K.-P. (1997). Eye position effects in monkey cortex. I. Visual and pursuit-related activity in extrastriate areas MT and MST. *Journal of Neurophysiology, 77*, 944–961.

Bremmer, F., Pouget, A., & Hoffmann, K.-P. (1998). Eye position encoding in the macaque posterior parietal cortex. *European Journal of Neuroscience, 10*, 153–160.

Bruce, C. J., Goldberg, M. E. (1985). Primate frontal eye fields. I. Single neurons discharging before saccades. *J. Neurophysiol., 53*, 603–635.

Buneo, C. A., Jarvis, M. R., Batista, A. P., & Andersen, R. A. (2002). Direct visuomotor transformations for reaching. *Nature, 416*, 632–636.

Campos, M., Cherian, A., & Segraves, M. A. (2006). Effects of eye position upon activity of neurons in macaque superior colliculus. *Journal of Neurophysiology, 95*, 505–526.

Cassanello, C., & Ferrera, V. P. (2005). *Eye position signals and vector subtraction in FEF neurons*. Society for Neuroscience abstract.

Colby, C. L., Duhamel, J. R., & Goldberg, M. E. (1995). Oculocentric spatial representation in parietal cortex. *Cerebral Cortex, 5*, 470–481.

Crawford, J. D., & Guitton, D. (1997). Visual-motor transformations for accurate and kinematically correct saccades. *Journal of Neurophysiology, 78*, 1447–1467.

Crawford, J. D., Medendorp, W. P., & Marotta, J. J. (2004). Spatial transformations for eye-hand coordination. *Journal of Neurophysiology, 92*, 10–19.

DeSouza, J. F. X., Dukelow, S. P., Gati, J. S., Menon, R. S., Andersen, R. A., & Vilis, T. (2000). Eye position signal modulates a human parietal pointing region during memory-guided movements. *Journal of Neuroscience, 20*, 5835–5840.

Duhamel, J. R., Colby, C. L., & Goldberg, M. E. (1992). The updating of the representation of visual space in parietal cortex by intended eye movements. *Science, 255*, 90–92.

Funahashi, S., & Takeda, K. (2002). Information processes in the primate prefrontal cortex in relation to working memory processes. *Reviews in the Neurosciences, 12*, 313–345.

Goldberg, M. E., & Bruce, C. J. (1990). Primate frontal eye fields. III. Maintenance of a spatially accurate saccade signal. *Journal of Neurophysiology, 64*, 489–508.

Henriques, D. Y. P., Klier, E. M., Smith, M. A., Lowy, D., & Crawford, J. D. (1998). Gaze-centered remapping of remembered visual space in an open-loop pointing task. *Journal of Neuroscience, 15*, 1583–1594.

Klier, E. M., & Crawford, J. D. (1998). Human oculomotor system accounts for 3-D eye orientation in the visual-motor transformation for saccades. *Journal of Neurophysiology, 80*, 2274–2294.

Medendorp, W. P., Smith, M. A., Tweed, D. B., & Crawford, J. D. (2002). Rotational remapping in human spatial memory during eye and head motion. *Journal of Neuroscience, 22*, RC196.

Misslisch, H., Tweed, D., & Vilis, T. (1998). Neural constraints on eye motion in human eye-head saccades. *Journal of Neurophysiology, 79*, 859–869.

Mitchell, J. F., & Zipser, D. (2003). Sequential memory-guided saccades and target selection: A neural model of the frontal eye fields. *Vision Research, 43*, 2669–2695.

Mullette-Gillman, O. A., Cohen, Y. E., & Groh, J. M. (2005). Eye-centered, head-centered, and complex coding of visual and auditory targets in the intraparietal sulcus. *Journal of Neurophysiology, 94*, 2331–2352.

Mushiake, H., Fujii, N., & Tanji, J. (1999). Microstimulation of the lateral wall of the intraparietal sulcus compared with the frontal eye field during oculomotor tasks. *Journal of Neurophysiology, 81*, 1443–1448.

Mushiake, H., Tanatsugu, Y., & Tanji, J. (1997). Neuronal activity in the ventral part of premotor cortex during target-reach movement is modulated by direction of gaze. *Journal of Neurophysiology, 78*, 567–571.

Pouget, A., Fisher, S. A., & Sejnowski, T. J. (1993). Egocentric spatial representation in early vision. *Journal of Cognitive Neuroscience, 5*, 150–161.

Pouget, A., & Sejnowski, T. J. (1997). Spatial transformations in the parietal cortex using basis functions. *Journal of Cognitive Neuroscience, 9*, 222–237.

Pouget, A., & Snyder, L. H. (2000). Computational approaches to sensorimotor transformations. *Nature Neuroscience, 3*, 1192–1198.

Quaia, C., & Optican, L. M. (1998). Commutative saccadic generator is sufficient to control a 3-D ocular plant with pulleys. *Journal of Neurophysiology, 79*, 3197–3215.

Quaia, C., Optican, L. M., & Goldberg, M. E. (1998). The maintenance of spatial accuracy by the perisaccadic remapping of visual receptive fields. *Neural Networks, 11*, 1229–1240.

Robinson, D. A., & Fuchs, A. F. (1969). Eye movements evoked by stimulation of frontal eye fileds. *Journal of Neurophysiology, 32*, 637–648.

Russo, G. S., & Bruce, C. J. (1993). Effect of eye position within the orbit on electrically elicited saccadic eye movements: A comparison of the macaque monkey's frontal and supplementary eye fields. *Journal of Neurophysiology, 69*, 800–818.

Salinas, E., & Abbott, L. F. (1995). Transfer of coded information from sensory to motor networks. *Journal of Neuroscience, 15*, 6461–6474.

Salinas, E., & Abbott, L. F. (1996). A model of multiplicative neural responses in parietal cortex. *Proc. Natl. Acad. Sci. USA, 93*, 11956–11961.

Salinas, E., & Abbott, L. F. (1997). Invariant visual responses from attentional gain fields. *Journal of Neurophysiology, 77*, 3267–3272.

Siegel, R. M. (1998). Representation of visual space in area 7a neurons using the center of mass equation. *Journal of Computational Neuroscience, 5*, 365–381.

Smith, M. A., & Crawford, J. D. (2001). Implications of ocular kinetics for the internal updating of visual space. *Journal of Neurophysiology, 86*, 2112–2117.

Snyder, L. H. (2000). Coordinate transformations for eye and arm movements in the brain. *Current Opinion Neurobiology, 10*, 747–754.

Tweed, D. (1997). Three-dimensional model of the human eye-head saccadic system. *Journal of Neurophysiology, 77*, 654–666.

Tweed, D., Haslwanter, T., & Fetter, M. (1998). Optimising gaze control in three dimensions. *Science, 281*, 1363–1366.

Umeno, M. M., & Goldberg, M. E. (1997). Spatial processing in the monkey frontal eye field. I. Predictive visual responses. *J. Neurophysiol., 78*(3), 1373–1383.

Van Opstal, A. J., Hepp, K., Suzuki, Y., & Henn, V. (1995). Influence of eye position on activity in monkey superior colliculus. *Journal of Neurophysiology, 74*, 1593–1610.

Walker, M. F., Fitzgibbon, E. J., & Goldberg, M. E. (1995). Neurons in the monkey superior colliculus predict the visual result of impending saccadic eye movements. *Journal of Neurophysiology, 73*, 1988–2003.

Xing, J., & Andersen, R. A. (2000). Memory activity of LIP neurons for sequential eye movements simulated with neural networks. *Journal of Neurophysiology, 84*, 651–665.

Zipser, D., & Andersen, R. A. (1988). A back-propagation programmed network that simulate response properties of a subset of posterior parietal neurons. *Nature, 331*, 679–684.

Received November 8, 2005; accepted November 1, 2006.